Biophysical Journal Volume 75 July 1998 493–502

Partition and Permeation of Dextran in Polyacrylamide Gel

James C. Williams, Jr., Lawrence A. Mark, and Susan Eichholtz
Department of Anatomy, Indiana University School of Medicine, Indianapolis, Indiana 46202-5120 USA

ABSTRACT Partition of sized FITC-dextrans in polyacrylamide gel showed a relationship between K_{av} and solute radius as predicted by the theory of Ogston, which is based solely on geometry of the spaces. Permeability data for the same dextrans were fit to several theories, including those based on geometry and those based on hydrodynamic interactions, and the gel structure predicted by the partition and permeability data were compared. The Brinkman effective-medium model (based on hydrodynamic interactions and requiring a measure of the hydraulic conductivity of the matrix) gave the best fit of permeability data with the values for fiber radius (r_f) and void volume of the gel (ϵ) that were obtained from the partition data. The models based on geometry and the hydrodynamic screening model of Cukier, using the r_f and ϵ from partition data, all predicted higher rates of permeation than observed experimentally, while the effective-medium model with added term for steric interaction predicted lower permeation than that observed. The size of cylindrical pores appropriate for the partition data predicted higher rates of permeation than observed. These relative results were unaffected by the method of estimating void volume of the gel. In sum, it appears that one can use data on partition of solute, combined with measurement of hydraulic conductivity, to predict solute permeation in polyacrylamide gel.

INTRODUCTION

Understanding the movement of macromolecules through matrices is important for many biological phenomena, including the reduced diffusion that occurs in cytoplasm (Jones and Luby-Phelps, 1996) and the restricted permeation of proteins across basement membranes (Williams, 1994). Much information has been gained by modeling such matrices as containing cylindrical pores (Deen et al., 1985), but recently interest has been shown in various forms of fiber-matrix models, which provide a closer match to the ultrastructure of biological matrices and polymer gels (Curry and Michel, 1980; Katz, 1992; Schnitzer, 1992; Katz and LaMarche, 1994; Phillips et al., 1989).

The classic derivation of the fiber-matrix model is that of Ogston, who used a geometric argument to gain expressions for the partition (Ogston, 1958) and diffusion (Ogston et al., 1973) of spheres in a matrix made of infinitely long, stiff rods. Other derivations of this same system are by Schnitzer (1988), who used a statistical mechanics approach and found expressions that differ from the Ogston theory under certain conditions (Schnitzer, 1992), and by Johansson and Löfroth (1993), who provide expressions that are valid for matrices made up of moderately flexible rods.

Besides these models based on geometric arguments, at least three theories have been proposed that take into account the hydrodynamic interactions that will occur between solute and matrix during diffusion. Cukier (1984) used expressions of hydrodynamic screening to describe the reduction of solute diffusion within a solution of polymers, while Tong and Anderson (1996) and Johnson et al. (1996) have applied different forms of the Brinkman effective medium model to describe the reduction of solute diffusion in gels. While the geometric models above require knowledge only of the radius and density of fibers in the matrix, the Cukier hydrodynamic screening approach requires additional knowledge of the ratio of fiber length to fiber radius, and the effective medium model requires knowledge of the Darcy permeability of the matrix.

Some experimental tests of these theories have been carried out in chromatographic beads and in polymer gels. For protein diffusing in AcA-34 (polyacrylamide) chromatographic beads, the Ogston fiber-matrix theory has been shown to be self-consistent in its predictions of partition and diffusion (Moussaoui et al., 1991), while similar work in agarose beads suggests that Ogston theory is not self-consistent in these systems, as diffusion of proteins was slower than would be predicted from solute partition data (Moussaoui et al., 1992; Johnson et al., 1995). In polymer gels, both agarose (Johnson et al., 1996) and polyacrylamide (Tong and Anderson, 1996) gels have been studied; while the two studies agreed that the Ogston theory was inaccurate in predicting diffusion rates, they disagreed as to which formulation of effective medium theory was best for fitting diffusion data for proteins, and the data for linear polymers did not match those for proteins (Tong and Anderson, 1996).

A complication in all of these studies is the assumptions made concerning the relevant sizes of molecules. When a theory requires a solute radius or volume, several methods are available for measuring this parameter, but not all give equivalent values. For example, Minton (1980) points out that various measures for molecular volume (such as partial specific and hydrodynamic volumes) do not necessarily reflect the functionally relevant volumes for molecular in-

Received for publication 25 June 1997 and in final form 27 March 1998.
Address reprint requests to James C. Williams, Jr., Department of Anatomy, Indiana University School of Medicine, 635 Barnhill Drive, Indianapolis, IN 46202-5120. Tel.: 317-274-3423; Fax: 317-278-2040; E-mail: williams@anatomy.iupui.edu.
Notes 1 and 2 appear at the end of the Conclusions section.

0006-3495/98/07/493/10 $2.00

teraction. In the studies cited above, the radius of permeating or partitioning solute has usually been assumed to be the Stokes radius calculated from diffusion determinations. While this may be appropriate for hard, spherical molecules, such as certain globular proteins, it is not appropriate for other molecules, such as sugar polymers; even for a spherical polymer like Ficoll, the Stokes radius (r_s) and the radius apparent from size-exclusion chromatography (r_{sec}) are not equivalent (Oliver et al., 1992). For matrices, matrix fiber radius (or volume) has sometimes been calculated from predicted molecular dimensions (e.g., from x-ray scattering), and sometimes from partial specific volumes, and it is not clear whether either of these approaches is appropriate.

In the present study we take the approach that r_{sec} is a reasonable measure of the size of the diffusing/partitioning molecule for any steric interactions, as such interactions predominate in size-exclusion chromatography (Hussain et al., 1991). Using this, we find agreement between partition and permeation data in polyacrylamide gel using the Brinkman effective medium model for predicting diffusion in the gel. To calculate the void volume of the gel (ϵ), we used the dry weight combined with the partial specific volume of polyacrylamide, but we find that the method used for estimation of ϵ did not affect the relative results among the different theories, but only alters the apparent value of the fiber radius.

METHODS

Polyacrylamide and dextrans

Polyacrylamide gels were prepared as for electrophoresis using typical methods. Briefly, stock solutions of electrophoresis-grade acrylamide and bis-acrylamide (C = 2.6%; both from Sigma Chemical, St. Louis, MO) were prepared in water, and an appropriate volume of stock solution was added to tris-buffered saline (1.5 M, pH = 8.8) and the mixture was degassed. Then ammonium persulfate and tetramethylenediamine (each 0.05%) were added to initiate polymerization. Gels were cast between glass plates and allowed to polymerize for at least 1 h. Gel slabs were then rinsed in water, and 20-mm-diameter disks were cut from the slabs using an arch cutter.

FITC-labeled dextrans (mixture of five polydisperse preparations, of M_w in thousands of 4, 20, 70, 150, and 500; all from Sigma Chemical) were fractionated at room temperature on a Sephacryl S-300HR column, 2.5 cm in diameter, with a packed bed height of 48 cm. The buffer was 0.05 M ammonium acetate (pH = 7) and the flow rate was maintained at 2.0 ml/min using a Bio-Rad EP-1 pump, taking 4-ml fractions. Only ~15 mg of mixed FITC-dextrans in ~0.3 ml was fractionated in a single run; this small sample size minimized spreading of elution peaks due to sample volume or viscosity. Each fractionation run was recorded using a UV monitor to ensure that fractions from different runs represented identical elution volumes. Each fraction was then pooled with identical fractions from other runs, and the dextrans were concentrated using a combination of Centriprep and Centricon concentrators (Amicon, Beverly, MA). Up to 80 ml of each fraction was concentrated to volumes as small as 0.2 ml. The amount of FITC-dextran in a fraction was determined by absorbance. Some fractions were run again on the column to check their degree of polydispersity, and the width of peaks was not greater than that for proteins; from the width of the peaks, M_w/M_n was estimated (conservatively) to be ≤ 1.08 for all fractions.

The molecular size of the dextrans in the fractions was determined by calibration with standard proteins (proteins, with assumed radii, were: cytochrome c, 17 Å; myoglobin, 19 Å; carbonic anhydrase, 22 Å; albumin, 35 Å; alcohol dehydrogenase, 46 Å; and β-amylase, 60 Å), and blue dextran was used for void volume determination. The molecular radius for an FITC-dextran fraction that was calculated from the protein standard curve reflects the functional size of the dextran. This radius, called r_{sec}, was used for predicting partition and permeation of the dextrans.

For linear polymers like dextran, r_{sec} is not necessarily the same as the Stokes radius, r_s, that is calculated from diffusion determinations. For the present study we used a chromatography medium and buffer system identical to that used by Oliver et al. (1992), who measured both r_{sec} and r_s for dextrans. Fitting the data from Fig. 6 in Oliver et al. to a polynomial, we find (in Å) $r_s = 0.628 + 1.089 r_{sec} - 0.00044 r_{sec}^2$. Using this calculated r_s, the diffusion coefficient in free solution, D_{free}, was estimated for each dextran fraction using the Stokes-Einstein relation, $D_{free} = kT/(6\pi\rho r_s)$. The product of the Boltzmann constant and the absolute temperature, kT, was taken to be 4.1×10^{-14} erg (room temperature, 22°C), and the viscosity, ρ, was taken to be that of water, 0.8904 centipoise.

Determination of volume fraction available to solute (free space, or K_{av}) (See Note 1)

Individual disks of polyacrylamide gel, cast 1.0 mm thick, were measured for weight, diameter (using calipers), and thickness (using a micrometer), and incubated in 4 ml of phosphate-buffer saline (PBS, consisting of 150 mM NaCl with 20 mM sodium phosphates, pH = 7.4; some experiments also had 0.02% sodium azide in the PBS with no apparent effect) containing FITC-dextran at a concentration of ~50 μg/ml, in capped, 20-ml glass vials. The vials were put on a shaker at low speed for 48 h at room temperature. At the end of this incubation period, each disk was removed from its vial, measured for weight, diameter, and thickness, and transferred to 2 ml of PBS for a rinsing period of 48 h. At the end of the rinsing period, each disk was removed, measured for diameter and thickness, and transferred to a tared vial for determination of final wet and dry weights. Some disks received an additional 2-h rinse in water before determination of wet and dry weights, which eliminated the need to correct the dry weights for salt content. Values for K_{av} were determined from measurements of total fluorescence (using a Turner fluorometer) in samples taken from the incubation and rinse solutions, corrected for carry-over volume (volume clinging to the outside of the gel), which was calculated from the apparent K_{av} for very large dextrans (radius > 100 Å). Carry-over volume was not significantly different (by multiple ANOVA) for different batches of gel, for different fractions of dextran used, or for different gel concentrations (%), and averaged ~2% of the disk volume (carry-over volume = 0.0091 ± 0.0006 ml for 27 batches of gel disks of average total volume 0.402 ± 0.002 ml).

Fit of K_{av} to theory

Given a void volume ratio of ϵ and a fiber radius of r_f, the volume of the gel available to a spherical solute of radius r_{sol} is

$$K_{av} = \exp\left[(\epsilon - 1)\left(1 + \frac{r_{sol}}{r_f}\right)^{\nu}\right] \quad (1)$$

where ν is a scaling parameter that can be related to the stiffness of the fiber (Johansson and Löfroth, 1993). For $\nu = 2$, Eq. 1 is the same as that derived by Ogston (Ogston et al., 1973; Ogston, 1958), and the same can also be obtained from Eq. 6.9 in Curry (1984). The equivalent equation for K_{av} derived by Schnitzer (1988) is slightly different:

$$K_{av} = \exp(\epsilon - 1)\exp\left\{\frac{(1-\epsilon)\left[1 - \left(\frac{r_{sol} + r_f}{r_f}\right)^2\right]}{\epsilon}\right\}. \quad (2)$$

Each of these equations describes a relationship between K_{av} and r_{sol} that is dependent on the values ϵ and r_f. Data for K_{av} obtained using a single

batch of polyacrylamide and incubating with solutes of different sizes were fit to Eqs. 1 and 2. Fits were obtained both by varying ϵ and r_f, or by varying r_f alone and using ϵ estimated from the mean fractional water content for that batch of polyacrylamide.

Partition data were also fit to single-radius pore theory, in which the volume of the gel available to a solute depends on the radius of the pore, r_p:

$$K_{av} = \epsilon\left(1 - \frac{r_{sol}}{r_p}\right)^2. \quad (3)$$

Permeation through gels

Disks of polyacrylamide gel, 0.5 mm thick, were prepared as above and soaked overnight in PBS (to allow for the same, slight swelling observed in the gels used for K_{av} determination). A disk was then mounted vertically between two halves of a lucite chamber, such that a 1-cm-diameter portion of the gel disk separated the two 4-ml compartments of the chamber. Each compartment was filled with PBS, and FITC-dextran was added to one of the compartments. The chamber was placed on a magnetic stirrer and both compartments were vigorously stirred using fluted stir-disks. Samples were taken from both compartments hourly, and fluorescence determined later. The measured concentration on the side to which FITC-dextran was initially added was always much greater than the concentration in the other compartment, so that the concentration difference across the gel was effectively constant throughout the experiment. Permeability was calculated as the rate of permeation divided by the product of the surface area of the gel and the concentration difference between the compartments.

The thickness of unstirred layers bounding the gel in the diffusion apparatus was estimated by measuring the permeation of FITC-glycine, which was prepared by mixing FITC (>90%, isomer I, from Sigma Chemical) with a molar excess of glycine. The unstirred layer thickness can be calculated from a measured permeability if the diffusion coefficient for the solute within the gel, D, is known. One might assume that $D \rightarrow D_{free}$ for a small solute, but this is not at all certain, as the theories set forth below differ on this point. For this reason, the maximum thickness of gel plus unstirred layers was calculated as D_{free}/P, where P is the measured permeability of FITC-glycine across the gel. The results suggested that unstirred layer effects were minimal, so that P could be taken to be that of the gel alone. (See data and discussion below.)

Fit of permeation data to theory

The rate of permeation across the gel (J_s) can be described by

$$J_s = \frac{A}{\Delta x} K_{av} D \Delta C \quad (4)$$

where A is the surface area of the gel, Δx is the thickness, and ΔC is the concentration difference between the compartments (see Note 2). The permeability is therefore

$$P = \frac{K_{av} D}{\Delta x}. \quad (5)$$

For the Ogston fiber-matrix theory, we have the following [the "stochastic model" (Ogston et al., 1973; Curry, 1984)]:

$$D_{Ogston} = D_{free} \exp\left[-(1 - \epsilon)^{1/2}\left(1 + \frac{r_{sol}}{r_f}\right)\right] \quad (6)$$

where D_{free} is the diffusion coefficient in free solution, calculated as described above. Another analysis of diffusion based on the geometry of the fiber matrix is that of Johansson and Löfroth (1993), who modeled the fiber matrix as consisting of moderately flexible rods, and who predicted an effect on diffusion as follows:

$$D_{Johansson} = D_{free}[e^{-\alpha} + \alpha^2 e^{\alpha} E_1(2\alpha)] \quad (7)$$

where

$$\alpha = (1 - \epsilon)\left(1 + \frac{r_{sol}}{r_f}\right)^2 \quad \text{and} \quad E_1(2\alpha) = \int_{2\alpha}^{\infty}\left(\frac{e^{-u}}{u}\,du\right).$$

E_1, the exponential integral, was evaluated using the relation

$$E_1(2\alpha) \approx -0.57721 - \ln|2\alpha| - \sum_{i=1}^{30} \frac{(-2\alpha)^i}{i(i!)}$$

which was found to be valid for $2\alpha \leq 10$. This was a reasonable limit for the data in the present study, and taking the series out to only 30 terms kept the computation times for nonlinear fitting of combined Eqs. 5 and 7 to only several seconds.

Other workers have stressed hydrodynamic relations in theories for diffusion in fiber matrices. Cukier (1984) used hydrodynamic screening theory to predict the following:

$$D_{Cukier} = D_{free} \exp\left[-\frac{r_{sol}}{r_f}\sqrt{\frac{3(1 - \epsilon)}{\ln(L/b)}}\right] \quad (8)$$

where L/b is the ratio of the fiber length to fiber diameter. Thus, Eq. 8 requires knowledge of the length of the fibers in the matrix—a measurement not made in the present study—while Eq. 6 assumes only that $L \gg r_{sec}$. (Equation 7 assumes that the flexible fibers of the matrix are long and are stiff enough that the persistence length of the fiber is >10× the fiber radius.)

Effective medium models are also based on consideration of the hydrodynamic interactions of molecules (Johnson et al., 1996; Tong and Anderson, 1996). Tong and Anderson (1996) found good prediction of protein diffusion in polyacrylamide gel using the Brinkman result:

$$D_{Brinkman} = D_{free}\left(1 + \frac{r_{sol}}{\sqrt{\kappa}} + \frac{1}{3}\left(\frac{r_{sol}}{\sqrt{\kappa}}\right)^2\right)^{-1} \quad (9)$$

where κ is the Darcy permeability of the matrix. In contrast, Johnson et al. (1996) fit diffusion in agarose gels using Eq. 9 that was modified to include a term that accounted for steric hindrance in the gel; the steric term used was the empirical relationship described by Johansson and Löfroth (1993), and with this D, is predicted by

$$D_{Brinkman+steric\ term} = D_{free}\left(1 + \frac{r_{sol}}{\sqrt{\kappa}} + \frac{1}{3}\left(\frac{r_{sol}}{\sqrt{\kappa}}\right)^2\right)^{-1} \exp[-0.84\alpha^{1.09}]. \quad (10)$$

Both Eqs. 9 and 10 require knowledge of κ, an expression of the hydraulic conductivity of the gel. The hydraulic conductivity of polyacrylamide gel was measured by Tokita and Tanaka (1991). For their 10% gels (with cross-linker concentration of 2%, similar to our concentration of 2.6%), the measured frictional coefficient was 9×10^{11} dyn · s · cm^{-4}. Dividing this value into the viscosity of water gives $\kappa = 99$ Å^2. Alternatively, Tong and Anderson (1996) used other data in the literature to obtain the relationship $\kappa = 2.64(\text{VolFract})^{-1.42}$, where VolFract is the volume fraction of the monomer before polymerization. For 10% gels in the present study, at 0.7 ml/g (Tong and Anderson, 1996), this gives a value of $\kappa = 115$ Å^2. The value of κ has a significant effect on the predictions of Eqs. 9 and 10, so both of these values were used and compared in the present study.

For pore theory, the predicted value for D is

$$D_p = D_{free}(1 - 2.10444\mu + 2.08877\mu^3 - 0.94813\mu^5 - 1.372\mu^6 + 3.87\mu^8 - 4.19\mu^9) \quad (11)$$

where $\mu = r_{sol}/r_p$ [as in Curry, Eq. 5.16 (Curry, 1984); this formula is valid only for $\mu \leq 0.6$].

Phenomenological descriptions of solute diffusion through matrix have been proposed that depend only on the void volume of the matrix and not the fiber (or pore) size. Lauffer (1961) described diffusion through agarose gels using

$$D_{Lauffer} = D_{free}\frac{1 + \beta(\epsilon - 1)}{\epsilon} \quad (12)$$

where β is a constant. Ogston et al. (1973) derived a different relationship:

$$D_{Og-phenom} = D_{free}\left[\frac{1}{1 + \gamma(1 - \epsilon)}\right]^2, \quad (13)$$

again, where γ is a constant. Eq. 13 was initially described as being unsuccessful in accurately describing the diffusion of solutes through polymers (Ogston et al., 1973).

Statistics

Data were fit to theory using the nonlinear fitting routines in *JMP* (SAS Institute, Cary, NC). Starting values for parameters were varied to confirm stable convergence in all cases. Confidence intervals were calculated in *JMP* using the likelihood method (Rivers et al., 1996). Where appropriate, data were compared using ANOVA or the Tukey-Kramer HSD test, and differences were considered significant if $p < 0.05$.

RESULTS

Partition of dextran in gels

Data from three sets of gels are shown in Fig. 1, which demonstrates the expected result that solute partition is more restricted in the gels of higher concentration. This was apparent even at the dextran of 87 Å radius, in which the data for Fig. 1 had K_{av} values of 0.036 ± 0.001, 0.012 ± 0.001, and 0.0014 ± 0.0001 for the 6, 8, and 10% gels, respectively, significantly decreasing with increasing concentration of gel. The dextran fraction at 132 Å radius was used for correcting these gels for carry-over volume (that is, K_{av} for the 132 Å fraction was assumed to be zero). Mean volume of the 132 Å fraction was 0.0082 ± 0.0002 ml (n = 9 gel disks), and mean gel total volume was 0.400 ± 0.005 ml (n = 18). A summary of all partition data is shown in Table 1.

The curve fits in Fig. 1 assume that the void volume of the gel, ϵ, can be estimated from the measured water fractions of the gels. For this calculation, the specific volume of polyacrylamide that was measured by Munk et al. (1980), 0.687 ml/g, was used (Tong and Anderson, 1996). Using these estimates of ϵ, the data were fit using Eq. 1, with ν = 2, and the fiber radii for the three curves were 7.5, 8.1, and 7.8 Å for the 6, 8, and 10% gels, respectively. That is, data from each of the three gel concentrations were best fit with curves that suggest a similar fiber size for all three gel concentrations.

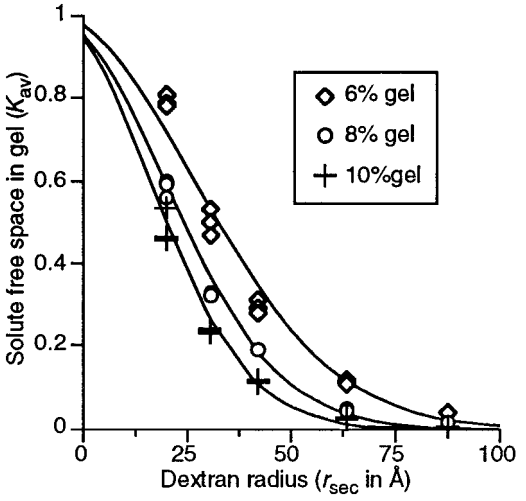

FIGURE 1 Solute free space (K_{av}) measured for three different concentrations of polyacrylamide gel using the same fractions of FITC-dextran and experiments carried out within the same week. Two or three gel disks were measured for each size of solute radius with each gel concentration. (Symbols are for individual measurements, and often overlap.) 6% gel: curve shows one-parameter fit with ϵ = 0.975 from water content, with data fitting best to r_f = 7.5 Å; two-parameter fit (not shown), void volume (ϵ) = 1.0, and fiber radius (r_f) = 0.3 Å. 8% gel: ϵ = 0.955 from water content, one-parameter fit, r_f = 8.1 Å; two-parameter fit (not shown), ϵ = 0.95 and r_f = 8.6 Å. 10% gel: ϵ = 0.945 from water content, one-parameter fit, r_f = 7.8 Å; two-parameter fit (not shown), ϵ = 0.94 and r_f = 8.1 Å.

Similar fits were obtained with the data from Table 1, as shown in Table 2. The one-parameter fit, shown at the far right of Table 2, is similar to the curves shown in Fig. 1, where ϵ was calculated from dry weights, and one can see that the pooled data suggest a fiber radius for the acrylamide that is quite similar for all of the gel concentrations. For the two-parameter fits shown in Table 2, the best-fit values for ϵ were not too far off from those calculated from dry weight data, but it is clear that using such partition data, even with as many data points as used in Table 2, to obtain both ϵ and r_f could lead to considerable error in estimation of both parameters.

The effect of varying ν, the scaling factor in Eq. 1, on the predicted value for fiber radius is shown in Fig. 2 for 6, 8, and 10% gels; ϵ is calculated from dry weights, as in Table 2. As ν is reduced, the partition data are fit by smaller values of the fiber radius. However, lower values of ν predict a flatter relationship between K_{av} and solute radius than is seen in the data, as shown in Fig. 3, where the effect of different values of ν *is* shown for pooled data from the partition of dextran into 10% gels. Note that curves fit using lower values for ν do not fit the "corner" of the data in the range of 30–90 Å solute radius as well as the curve does with ν = 2.

Comparison of fits of the partition data between the Ogston and Schnitzer theories (Eqs. 1 and 2) can be made

TABLE 1 Data for partition of FITC-dextran into polyacrylamide gel

Dextran radius (Å)	Fractional volume of gel available to dextran (K_{av})		
	6% Gels	8% Gels	10% Gels
15.1	0.77 ± 0.02 (29)	0.71 ± 0.02 (13)	0.59 ± 0.03 (15)
16.8	0.66 ± 0.03 (10)	0.59 ± 0.02 (3)	0.49 ± 0.02 (3)
18.6	0.76 ± 0.01 (6)	0.70 ± 0.02 (24)	0.68 ± 0.03 (23)
20.6	0.79 ± 0.01 (3)	0.58 ± 0.03 (13)	0.47 ± 0.03 (7)
22.9	0.66 ± 0.02 (20)	—	0.42 ± 0.01 (8)
25.4	0.51 ± 0.02 (10)	—	—
31.2	0.45 ± 0.02 (6)	0.39 ± 0.01 (30)	0.30 ± 0.01 (30)
34.6	0.47 ± 0.01 (35)	0.28 ± 0.016 (13)	0.32 ± 0.02 (21)
42.5	0.32 ± 0.02 (13)	0.19 ± 0.001 (3)	0.11 ± 0.001 (3)
52.2	0.29 ± 0.004 (6)	—	—
64.2	0.11 ± 0.003 (3)	0.065 ± 0.0055 (23)	0.02 ± 0.004 (27)
71.1	0.11 ± 0.002 (4)	—	—
87.4	0.037 ± 0.0007 (21)	0.012 ± 0.001 (9)	0.006 ± 0.0006 (12)
119*	−0.00003 ± 0.001 (4)	—	—
132*	−0.000005 ± 0.0004 (3)	−0.00003 ± 0.0005 (17)	−0.00006 ± 0.0004 (19)
147*	−0.0008 ± 0.0004 (41)	—	0.0001 ± 0.0003 (10)
>162*#	0.0002 ± 0.0002 (3)	0.002 ± 0.002 (17)	−0.0007 ± 0.0007 (14)

Dextran radius is mean apparent radius from size-exclusion chromatography. Values of K_{av} are shown as mean ± SE, with number of gel disks measured shown in parentheses. Gel % is nominal value only; actual content of final gels (by dry weight) was less than nominal (e.g., in 10% gels, fractional water content averaged 0.9199 ± 0.0003 for 56 gel disks).

*These dextran fractions were used for correcting for carry-over volume; for each day's experiment, one of these fractions was used for two or more disks, and mean K_{av} for this fraction was assumed to be zero. See text for explanation of carry-over volume.

#This dextran fraction was at void volume of column, so stated radius is a minimum value.

by comparing Tables 2 and 3. Note that the fiber radii predicted using the Schnitzer equation were consistently larger than the radii predicted by the simpler Ogston equation. These differences are not great, but it is clear that the Schnitzer theory is consistent with thicker fibers (and thus less total length of fibers) within the matrix in comparison with the Ogston theory.

Permeation of dextrans across gels

Plots of the diffusional permeation of gel slabs by FITC-dextran were linear with time, and the concentration of FITC-dextran in its initial compartment did not change significantly over the time of the experiments. Thus, the rates of permeation were easily calculated, and were converted to permeability values (Table 4) for ease of fitting to model predictions, as shown in Fig. 4. The range of sizes of dextrans for permeation experiments was dictated by the method used: measurement of permeation of molecules larger than 30 Å radius was not practical, as the rate of permeation for larger molecules across the 0.5 mm gels was too slow for an experiment to be completed in one day. At the other end, accurate fractionation of molecules much below an r_{sec} of 15 Å was not possible on the column used.

Unstirred layer thickness was estimated by measuring the rate of permeation of FITC-glycine, a molecule small enough that its rate of diffusion in the gel should be little different from that in free solution. Mean permeability for FITC-glycine in 10% gels was $7.82 \pm 0.13 \times 10^{-5}$ cm/s ($n = 3$). Because $D_{free} \leq 5 \times 10^{-6}$ cm^2/s, the maximum thickness of the total unstirred slab in the chamber is 640 μm. This is not much larger than the nominal thickness of the gel (0.5 mm). Moreover, it is certain that the gel will have some effect on reducing diffusion (if only by reducing the total volume of fluid available to the solute), so that the actual thickness of the unstirred layer is apparently <70 μm on each side of the gel.

The increased restriction of permeation across 10% gels with increasing molecular size is easily seen in Fig. 4. This is a real effect of restriction to permeation across the gel, as a plot of P/D_{free} against r_{sec} (Katz and Schaeffer, 1991) showed a significant negative slope (plot not shown; slope was -0.27 cm^{-1}/Å radius, $p = 0.0015$).

Note that with the exception of the fit from Eqs. 12 and 13, the shape of the data in Fig. 4 is fit fairly well by all of the theories described in the Methods. The effective medium models fit the data with curves that have less slope than those predicted by the other models, with the Johansson geometric model having the steepest slope, but these differences are not large at any point. In contrast, the fiber

TABLE 2 Values of void volume (ϵ) and fiber radius (r_f) in polyacrylamide gels calculated from measurement of equilibrium content of sized FITC-dextrans

Gel %	Two-parameter fit			One-parameter fit
	ϵ	r_f (Å)	ϵ from dry wt	r_f (Å)
6	0.93 ± 0.01	14.1 ± 1.7	0.971	8.1 ± 0.1
8	0.97 ± 0.01	6.4 ± 1.3	0.956	8.6 ± 0.1
10	0.92 ± 0.02	11.4 ± 2.0	0.945	8.8 ± 0.1

Uses Eq. 1 with $\nu = 2$. For 6% gels, $n = 217$ data points from a total of 12 days of experiments (with a new batch of gel for each day); 8%, $n = 165$ data points from 9 days; 10%, $n = 192$ data points from 10 days.

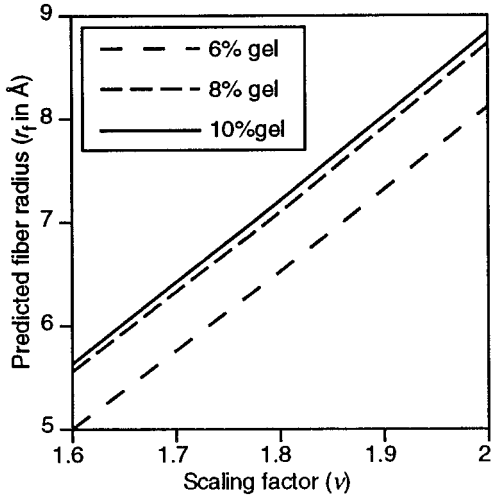

FIGURE 2 Effect of varying scaling factor (ν) in Eq. 1 on predicted value of fiber radius from data in Table 1. Note that the relationship is apparently linear, and that the data from 8 and 10% gels yield predicted fiber radii that are very close, while data from 6% gels suggest a slightly thinner fiber.

radius of the matrix that is consistent with these fits to the permeability data in Fig. 4 varies among these models, as shown in Fig. 5, which shows the predicted fiber radii from the partition experiments (using Eq. 1 and the data in Fig. 3) along with the predicted fiber radii using the different diffusion theories and the data in Fig. 4. The error bars show the 95% confidence intervals for the nonlinear fits. Note that this confidence interval is calculated assuming that the void volume of the gel is known exactly, so the true confidence intervals for the fiber radius will be larger than shown. However, this figure does allow a visual comparison of which analyses show consistent fits between the partition and permeation data.

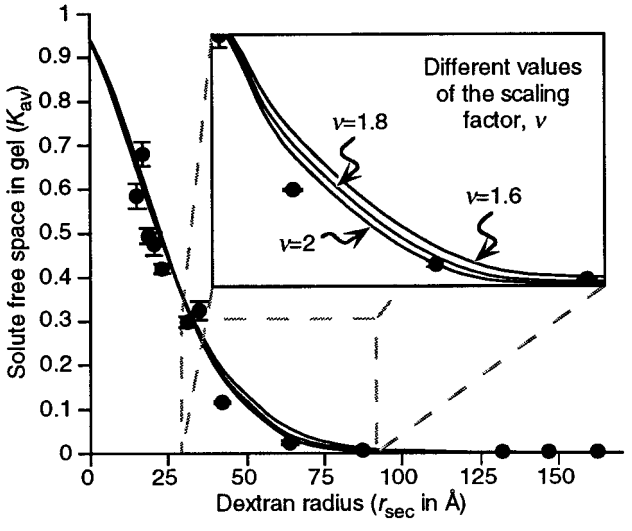

FIGURE 3 Pooled data on solute free space in 10% gels. Data are same as Table 1. Curve fits use the Ogston equation, Eq. 1, with different values for the scaling factor, ν. Note that $\nu = 2$ provides the best fit of the data.

TABLE 3 One-parameter fit of data in Table 2 using Schnitzer model of solute partition

Gel %	r_f (Å)
6	8.3 ± 0.1
8	8.8 ± 0.1
10	9.1 ± 0.2

Data are the same as in Table 2, but fit was made using Eq. 2, with ϵ values as calculated from dry weights and partial specific volume of polyacrylamide.

This comparison shows that the Brinkman effective medium model—with either of the two estimates for the Darcy constant—yielded a fit with the permeation data that is consistent with the partition data and a scaling factor of $\nu = 2$. The geometric models of permeation (Ogston, Schnitzer, and Johansson) and the hydrodynamic screening model of Cukier are consistent with ν in the range of 1.6–1.7; however, the shape of the partition data does not support the appropriate use of $\nu < 2$ (see above and Fig. 3). Varying the Cukier parameter of L/b did not change this greatly. The addition of a steric term to the Brinkman effective medium model fit the permeation data with fiber radii considerably larger than those predicted by the partition data.

Some of these fits are shown overlaid on the permeation data in the lower panel of Fig. 6, where the fiber radii consistent with the partition data are used for the calculations of permeation. Using these radii, the geometric theories predict a higher rate of permeation than was seen, while the effective medium model with steric term predicts a lower rate. Similarly, in the top panel of Fig. 6 it can be seen that the fiber radii consistent with the permeation data for the geometric theories predict K_{av} values that are lower than measured experimentally, while the effective medium model with added steric term yields predictions of K_{av} values that are too high.

The fit of partition and permeation data with pore theory is shown in Fig. 7. Note that pore theory is not self-consistent with regard to the data on partition and permeation of dextrans in the present study.

DISCUSSION

This study was motivated by a desire to find a consistent theoretical description of partition and permeation of mac-

TABLE 4 Data for diffusion of FITC-dextran across 0.5-mm-thick 10% polyacrylamide gel

Dextran radius (Å)	Permeability (10^{-6} cm/s)
15.1	6.61 ± 0.85 (3)
16.8	5.44 ± 0.61 (11)
18.6	4.44 ± 0.94 (3)
20.6	3.11 ± 0.64 (4)
22.9	2.36 ± 0.15 (2)
25.4	1.97 (1)
28.1	0.79 (1)

Values are shown as mean ± SE with number of gel disks measured shown in parentheses.

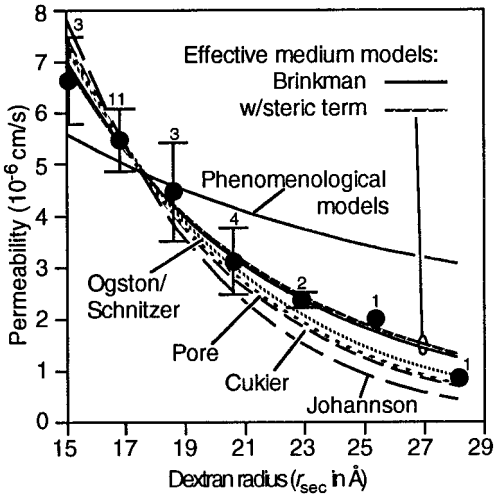

FIGURE 4 Permeability of FITC-dextran across 0.5-mm-thick 10% polyacrylamide gel. The number of gel pieces tested with each dextran fraction is shown by the numerals next to the symbols. Model fits all assume $\epsilon = 0.945$ and use Eqs. 1 (K_{av}, with $\nu = 2$) and 5 (P) unless stated otherwise: Ogston (Eq. 6), $r_f = 6.2$ Å; Schnitzer (Eqs. 2 and 6), $r_f = 6.4$ Å; Johansson (Eq. 7), $r_f = 5.3$ Å; Cukier (Eq. 8), $L/b = 10$, $r_f = 5.8$ Å; Brinkman (Eq. 9), $\kappa = 115$ Å^2, $r_f = 9.7$ Å; Brinkman with steric term (Eq. 10), $\kappa = 115$ Å^2, $r_f = 15.6$ Å; pore model (Eqs. 3 and 11), $r_p = 58.2$ Å; Lauffer phenomenological model (Eq. 12), $\beta = 14.9$; and Ogston phenomenological model (Eq. 13), $\gamma = 23.8$.

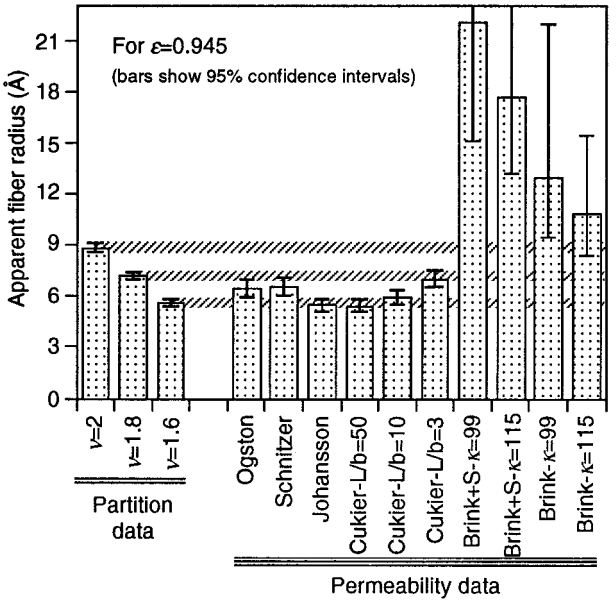

FIGURE 5 Predicted fiber radii in 10% gel using data in Figs. 3 or 4 and various models. Shown here are likelihood confidence intervals of apparent radius of fibers in gel for partition fits using Eq. 1 (Table 2 and Fig. 3) and for various theories for fitting permeability data (from Fig. 4). Confidence intervals for partition data are projected in the background with hatched bars so that intersection with confidence intervals of permeability data can be seen easily. Note that the partition fit with $\nu = 2$ is the best fit for partition data, and that the confidence interval for this fit falls within ranges of Brinkman fits ("Brink," Eq. 9). "Brink + S" is Brinkman effective medium model with steric term added (Eq. 10). All other designations are as in Fig. 4.

romolecules in a matrix. While equilibrium partition of solutes can be measured in many biological matrices (e.g., by quantitative immunostaining), measuring rates of permeation through a matrix is generally more difficult due to the anatomical arrangement of the tissue. Theoretically, one could measure the partition coefficients for a range of solute sizes to obtain a description of the physical characteristics of the matrix, and use that characterization to predict diffusion and permeability. This idea was tested in polyacrylamide gel as an easily handled model system.

The results suggest that, indeed, one can probe the physical nature of a matrix by measuring equilibrium partition of molecules—and the partition data in the present study (Fig. 3) matched the shape of the Ogston theory quite closely—and then accurately predict the ability of the molecules to permeate the matrix, but to do this one needs additional data: the hydraulic permeability of the matrix. That is, the best results for predicting permeation in the present study were found using the Brinkman effective-medium description of solute diffusion in a matrix (Fig. 6), and this description requires knowledge of the Darcy constant of the matrix.

This is a significant problem, as measuring the Darcy constant in some matrices (such as in cytoplasm or interstitial extracellular matrix) could be difficult. Moreover, the Darcy constant for a matrix as simple as polyacrylamide gel is not easy to measure; two different values were gleaned from the literature for the present study, and the results were quite different for the two values used. Finally, it must be noted that simply increasing the number of parameters in a model increases the chances of a good fit (Katchalsky, 1963), so one should view this result with some caution. Still, simple addition of an additional parameter, such as with the Cukier model, did not give as good a fit between the partition and diffusion data as did the Brinkman model, so there is good reason to think that the Brinkman model provides a better description of the interactions of diffusion within the gel than do the other theories.

The results found using other theories of solute permeation did well in describing the permeation data alone, with the exception of the so-called phenomenological equations 12 and 13, which did not fit the shape of the data (Fig. 4). Of course, all of the permeation calculations used K_{av} as calculated from Ogston's formulation (Eq. 1) in fitting permeability (Eq. 5), so that the differences in fit among models were due to estimation of the diffusion coefficient for the solutes within the gel. (The single exception to this is the Schnitzer values in Fig. 5, which used Eq. 2 for K_{av}, but these were very close to the Ogston values.) Over the range of values of solute radius shown in Fig. 4, K_{av} ranged from 0.4 to 0.7 (for $r_f = 8.8$ Å), indicating that K_{av} alone would reduce permeability in the 10% gel to about half of that in free solution for this range of solute sizes. For the Ogston theory, reduction of D in the gel was comparable to this: with $r_f = 8.8$ Å, $K_{av}/(D/D_{free})$, that is, the ratio of the reduction due to K_{av} to the reduction due to D, averaged 1.3

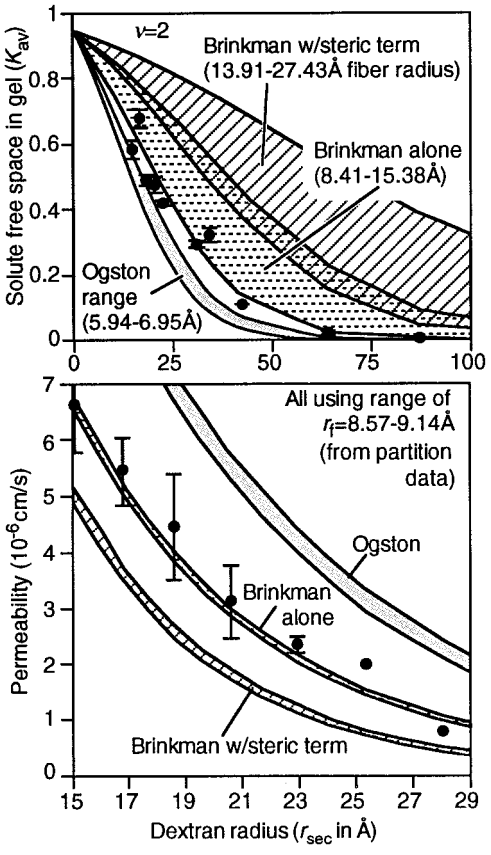

FIGURE 6 Visual comparison of partition and permeability fits for data in 10% gels. *Top:* Using the 95% confidence intervals for fiber radius (r_f) from fit of the permeability data, these values are plugged into Eq. 1 to show predicted ranges of solute partition. Three theories are designated, as in Fig. 4. Note that the range from the Brinkman theory overlaps most partition data points. *Bottom:* In reverse of above, here confidence interval values for r_f that fit partition data (with $\nu = 2$) are compared. Note that by using r_f predicted by partition data, Brinkman theory (with $\kappa = 115$ Å^2) fits permeability data very well. $\epsilon = 0.945$ for all.

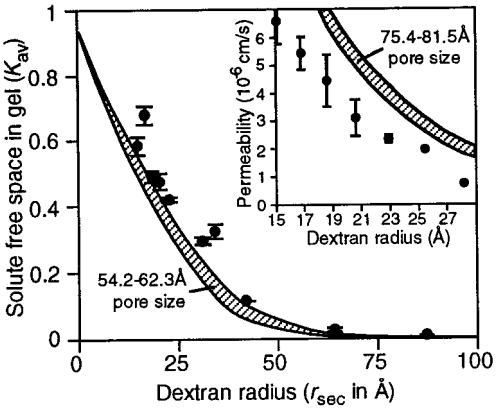

FIGURE 7 Visual comparison of partition and permeability fits from pore theory for data in 10% gels. The main panel shows predicted partition from fit of permeability data. *Inset:* predicted permeability range calculated using pore size confidence interval from fit of partition data.

for the solute range of Fig. 4. However, with the Brinkman effective-medium model, $K_{av}/(D/D_{free})$ averaged 2.2, indicating the relatively smaller diffusion coefficient in the gel predicted by this model.

These results, showing comparison of partition and permeation data, are similar to those found by Tong and Anderson (1996) for proteins in polyacrylamide gel. They found that the Brinkman model described diffusion rates in the gel accurately, just as the use of the Brinkman model fit the permeation data in the present study. However, they found that this result was valid only for proteins, and not for polyethylene glycol, which, like the dextran used in the present study, is a linear polymer. Polyethylene glycol diffusion did vary with gel concentration, but the measured diffusion constants were greater than those predicted by the Brinkman model and the two sizes of polymer did not differ in their diffusion constants within the gel, whereas protein diffusion was fit accurately by the model and showed appropriate differences in diffusion for the two proteins used (Tong and Anderson, 1996). It is not clear why these results for polyethylene glycol were different from the dextran results in the present study, but it should be understood that the permeation measured in the present study is different from the diffusion measured by Tong and Anderson. Permeation includes both a partition and diffusion component. This difference, combined with the different methods of estimating solute and fiber radii in these two studies, makes it difficult to compare them directly.

A good fit of protein partition and diffusion was found by Johnson et al. (1995) with the Brinkman model in SP-Sepharose beads, but in agarose gels the same group found that the Brinkman model needed an additional steric term (Eq. 10) to fit the diffusion data (Johnson et al., 1996). In other chromatographic beads, Moussaoui et al. (1991) found that partition and diffusion of proteins was accurately described by the Ogston equations in the gel AcA-34, which is acrylamide-based, but not in Sepharose Cl-B, which is a cross-linked agarose gel (Moussaoui et al., 1992).

It is difficult to reconcile all of these studies. Even within the same matrix—acrylamide-based or agarose-based—the results are conflicting. Methodological differences could play a role in the differing results, although all of the studies just cited measured diffusion in the matrix using fluorescence recovery after photobleaching (FRAP). The present study is unique in this regard, as the method we used for measuring permeability is unaffected by solute binding to the gel, or by some solute being trapped as a relatively immobile fraction, both of which require correction in the FRAP method.

However, the method we used for measuring permeability *is* susceptible to error due to unstirred layers. In this method, diffusion of the dextran from one chamber to the other requires the dextran to penetrate the gel along with the unstirred layers of fluid bounding each surface of the gel. The error induced by the presence of these unstirred layers will vary according to the thickness of the layers and the permeability of the gel slab, and will be greatest for small solutes. Assuming unstirred layers of 100 μm thickness on

both sides of the gel (thicker than that estimated), the error in the permeability measurement would have averaged only 7.1 ± 0.6% over all of the data points in Table 4. Note that this error results in measured values that are smaller than the actual gel permeability, and so the points in Figs. 4, 6, and 7 would be slightly higher with this error taken into account, but errors this small would not affect the conclusions that were drawn.

Other studies have uniformly used the Stokes radii for molecules permeating and partitioning into matrices. The present study used r_{sec} for molecular size, and this is arguably the best choice for linear polymers, as the effects on partition and diffusion of the variable shape of the molecule will be present in both the chromatographic column and in the experiments with gels. Other studies have used various measurements for the void volume and fiber radius of the matrix. In the present study, the matrix void volume ratio was estimated using dry weights with the partial specific volume of polyacrylamide. One cannot be certain that this gives the correct void volume, but free fit of the pooled partition data (Table 2) yielded values for void volume that were not far from those calculated for 6 and 10% gels. Moreover, the overall results in the present study were unaffected by the way that void volume was estimated. If the partial specific volume of polyacrylamide was assumed to be 0.7, 1.0, or 1.3, the relative results came out the same, just with different values for the apparent fiber radius of the matrix.

Nature of the matrix

Some of the studies cited above used x-ray diffraction or similar data for the size of the fibers in the matrix. In the present study we assumed no dimensions, but simply looked to see whether the apparent dimensions of the matrix fibers matched between the partition and diffusion data. The apparent radius of the "fibers" in the polyacrylamide was just under 9 Å, which is reasonable; it is slightly larger than the 5.5–6.5 Å values suggested by Tong and Anderson (1996), but similar to the 8.6–9.0 Å radii found by Ogston et al. (1973).

Although polyacrylamide solution has been viewed as a model fiber matrix (Ogston et al., 1973), cross-linked polyacrylamide gel is not a matrix of randomly oriented rods (Tietz, 1988). Rather, the work of Rüchel and colleagues has shown that polyacrylamide gel consists of open "cells" surrounded by thin walls, rather like a sponge (Rüchel and Brager, 1975; Rüchel et al., 1978). These cells are large relative to solutes (several μm in diameter) while the walls may be quite thin.

Thus, a fiber-matrix analysis of solute interaction with polyacrylamide gel is mainly of functional use, rather than being a match to the exact geometry of the gel. Still, the fiber-matrix model is superior to an equivalent pore model, because an absolute limit to the size of molecule that permeates a gel, which is implicit in pore theory, was not consistent with the data in the present study. For example, when the data are fit using pore theory (Fig. 7), K_{av} for solutes with a radius of 87 Å is predicted to be zero, while the experimental values for K_{av}, though small, were significantly greater at 87 Å than at 132 Å. That is, the experimental data were not consistent with a pore radius smaller than 87 Å, even though the best fit of the pore theory to the data required such a small pore size. This deficit could have been remedied by using a heteroporous model (Deen et al., 1985), but such a model would have introduced yet another parameter into the analysis.

Ogston versus Schnitzer derivations of partition in fiber-matrix

The Ogston equation (Eq. 1 with $\nu = 2$) is derived using a geometric argument and by assuming that spaces of a given size are distributed within the matrix according to the Poisson distribution (Ogston, 1958). The Schnitzer equation (Eq. 2) is derived using a statistical physics approach and by assuming that the number of accessible spaces is predicted by a Gaussian distribution (Schnitzer, 1988). The difference between the two equations is most apparent at small values of the void volume ratio and large values of solute size (Schnitzer, 1992). As described above, fits using these two derivations of the theory did differ, but only minimally.

The conditions under which the two derivations yield widely different predictions—small ϵ and large r_{sec}—were not important for the present study. For example, for $\epsilon = 0.90$ and $r_{sol}/r_f \approx 7.0$, K_{av} predicted by Ogston is about twice that predicted by Schnitzer (1992). However, in the present study (Figs. 1 and 3), values of K_{av} at $r_{sol}/r_f \approx 7.0$ are so close to zero that the difference between the two derivations is of no significance. Similarly, the permeation data (Fig. 4) are for relatively small molecules ($r_{sol}/r_f < 4$), and permeabilities for large molecules would be extremely low, so the difference between fits of the two derivations is trivial. It would be good to compare the two derivations measuring permeation of very large molecules and compare these to the other models shown above, but such experiments are technically difficult. For most biological applications (for example, partition of soluble proteins into extracellular matrix, where $r_{sol}/r_f \leq \sim 1$) these two derivations of fiber-matrix theory are probably equally applicable.

CONCLUSIONS

The data in the present study show that it is presently not feasible to use partition data for predicting permeation of macromolecules in polyacrylamide gel without having additional data on the hydraulic conductivity of the gel. The Brinkman formulation for diffusion in a gel is superior to other models, but measuring the Darcy constant in biological matrices is technically very difficult. For work with biological matrices, it would be useful to have a model that accurately predicts solute permeation from partition data

alone, and perhaps this is a reasonable direction for future research.

NOTES

1. Here we follow Curry (1984) and use K_{av} and ϕ (the partition coefficient) as distinct from one another. K_{av} is the ratio of the equilibrium solute concentration in the gel relative to that in the incubation solution, calculating the gel concentration as the solute content divided by the gel volume. ϕ is the ratio of the concentration of the solute within the void volume of the gel relative to that in the incubation solution. As solute radius goes to zero, $\phi \rightarrow 1.0$, while $K_{av} \rightarrow \epsilon$, which is the void volume of the gel. (Note that $K_{av} \rightarrow \epsilon$ is true in Eqs. 1 and 2 only for values of $\epsilon \geq 0.9$; in general, Eqs. 1 and 2 predict $K_{av} \rightarrow e^{\epsilon-1}$, which is close to ϵ if ϵ is close to 1. This is a consequence of the assumption in fiber-matrix theory that the free space in the matrix is much greater than the volume occupied by the fibers, and means that these theories should be used with caution for values of $\epsilon < 0.9$.)

2. In Eqs. 4 and 5 we differ from Curry (1984) in using K_{av} in place of ϕ. The rationale for the use of K_{av} here is that the equations for D appear to be based on the entire volume of the gel (as explicitly described by Ogston et al., 1973), rather than just the fluid space represented by the void volume. Thus it is K_{av} that appropriately expresses the drop in solute concentration in moving from the bulk solution into the matrix. In the end, though, the conclusions of the present work are unchanged if ϕ, rather than K_{av}, is used in Eqs. 4 and 5.

We thank Drs. George Tanner and Judy Boyd-White for helpful discussion, and Dr. Paul Dubin for helpful criticism of the manuscript and for suggesting the use of r_{sec} in this analysis. We thank the reviewers for many excellent suggestions, including directing us to the appropriate use of K_{av} in Eqs. 4 and 5.

This work was funded by Juvenile Diabetes Foundation International Award 193201 and an Established Investigator Award from the American Heart Association (to J.C.W.).

REFERENCES

Cukier, R. I. 1984. Diffusion of Brownian spheres in semidilute polymer solutions. *Macromolecules*. 17:252–255.

Curry, F. E. 1984. Mechanics and thermodynamics of transcapillary exchange. *In* Handbook of Physiology. Sect. 2: The Cardiovascular System, Vol. IV. Microcirculation, Part 1. E. M. Renkin and C. C. Michel, editors. American Physiological Society, Bethesda. 309–374.

Curry, F. E., and C. C. Michel. 1980. A fiber matrix model of capillary permeability. *Microvasc. Res.* 20:96–99.

Deen, W. M., C. R. Bridges, B. M. Brenner, and B. D. Myers. 1985. Heteroporous model of glomerular size selectivity: application to normal and nephrotic humans. *Am. J. Physiol.* 249:F374–F389.

Hussain, S., M. S. Mehta, J. I. Kaplan, and P. L. Dubin. 1991. Experimental evaluation of conflicting models for size exclusion chromatography. *Anal. Chem.* 63:1132–1138.

Johansson, L., and J.-E. Löfroth. 1993. Diffusion and interaction in gels and solutions. 4. Hard sphere Brownian dynamics simulations. *J. Chem. Phys.* 98:7471–7479.

Johnson, E. M., D. A. Berk, R. K. Jain, and W. M. Deen. 1995. Diffusion and partitioning of proteins in charged agarose gels. *Biophys. J.* 68: 1561–1568.

Johnson, E. M., D. A. Berk, R. K. Jain, and W. M. Deen. 1996. Hindered diffusion in agarose gels: test of effective medium model. *Biophys. J.* 70:1017–1023.

Jones, J. D., and K. Luby-Phelps. 1996. Tracer diffusion through F-actin: effect of filament length and cross-linking. *Biophys. J.* 71:2742–2750.

Katchalsky, A. 1963. Nonequilibrium thermodynamics. *International Science and Technology*. Oct:43–49.

Katz, M. A. 1992. Structural change in fiber matrix allows for enhanced permeability and reduced hydraulic conductivity. *Microvasc. Res.* 43: 1–6.

Katz, M. A., and M. L. LaMarche. 1994. Fiber matrix descriptors from permeability data without requiring membrane thickness: theory, results, and optimization. *Microcirculation*. 1:111–119.

Katz, M. A., and R. C. Schaeffer, Jr. 1991. Convection of macromolecules is the dominant mode of transport across horizontal 0.4- and 3-μm filters in diffusion chambers: significance for biologic monolayer permeability assessment. *Microvasc. Res.* 41:149–163.

Lauffer, M. A. 1961. Theory of diffusion in gels. *Biophys. J.* 1:205–213.

Minton, A. P. 1980. Thermodynamic nonideality and the dependence of partition coefficient upon solute concentration in exclusion chromatography. Application to self-associating and non-self-associating solutes. Application to hemoglobin. *Biophys. Chem.* 12:271–277.

Moussaoui, M., M. Benlyas, and P. Wahl. 1991. Diffusion of proteins in the chromatographic gel AcA-34. *J. Chromatogr.* 558:71–80.

Moussaoui, M., M. Benlyas, and P. Wahl. 1992. Diffusion of proteins in Sepharose Cl-B gels. *J. Chromatogr.* 591:115–120.

Munk, P., T. M. Aminabhavi, P. Williams, D. E. Hoffman, and M. Chmelir. 1980. Some solution properties of polyacrylamide. *Macromolecules*. 13:871–875.

Ogston, A. G. 1958. The spaces in a uniform random suspension of fibres. *Trans. Faraday Soc.* 54:1754–1757.

Ogston, A. G., B. N. Preston, and J. D. Wells. 1973. On the transport of compact particles through solutions of chain-polymers. *Proc. R. Soc. Lond. A*. 333:297–316.

Oliver, J. D. III, S. Anderson, J. L. Troy, B. M. Brenner, and W. M. Deen. 1992. Determination of glomerular size-selectivity in the normal rat with Ficoll. *J. Am. Soc. Nephrol.* 3:214–228.

Phillips, R. J., W. M. Deen, and J. F. Brady. 1989. Hindered transport of spherical macromolecules in fibrous membranes and gels. *AIChE J.* 35:1761–1769.

Rivers, R. L., J. A. McAteer, J. L. Clendenon, B. A. Connors, A. P. Evan, and J. C. Williams, Jr. 1996. Apical membrane permeability of MDCK cells. *Am. J. Physiol. Cell Physiol.* 271:C226–C234.

Rüchel, R., and M. D. Brager. 1975. Scanning electron microscopic observations of polyacrylamide gels. *Anal. Biochem.* 68:415–428.

Rüchel, R., R. L. Steere, and E. F. Erbe. 1978. Transmission-electron microscopic observations of freeze-etched polyacrylamide gels. *J. Chromatogr.* 166:563–575.

Schnitzer, J. E. 1988. Analysis of steric partition behavior of molecules in membranes using statistical physics. Application to gel chromatography and electrophoresis. *Biophys. J.* 54:1065–1076.

Schnitzer, J. E. 1992. Fiber matrix model reanalysis: matrix exclusion limits define effective pore radius describing capillary and glomerular permselectivity. *Microvasc. Res.* 43:342–346.

Tietz, D. 1988. Evaluation of mobility data obtained from gel electrophoresis: strategies in the computation of particle and gel properties on the basis of the extended Ogston model. *Adv. Electrophor.* 2:109–169.

Tokita, M., and T. Tanaka. 1991. Friction coefficient of polymer networks of gels. *J. Chem. Phys.* 95:4613–4619.

Tong, J., and J. L. Anderson. 1996. Partitioning and diffusion of proteins and linear polymers in polyacrylamide gels. *Biophys. J.* 70:1505–1513.

Williams, J. C., Jr. 1994. Permeability of basement membranes to macromolecules. *Proc. Soc. Exp. Biol. Med.* 207:13–19.